

Voltage vulnerability curves

Data-driven dynamic security assessment of voltage stability and system strength in modern power systems

Boričić, Aleksandar; Popov, Marjan

DOI

[10.1016/j.ijepes.2025.110636](https://doi.org/10.1016/j.ijepes.2025.110636)

Publication date

2025

Document Version

Final published version

Published in

International Journal of Electrical Power and Energy Systems

Citation (APA)

Boričić, A., & Popov, M. (2025). Voltage vulnerability curves: Data-driven dynamic security assessment of voltage stability and system strength in modern power systems. *International Journal of Electrical Power and Energy Systems*, 168, Article 110636. <https://doi.org/10.1016/j.ijepes.2025.110636>

Important note

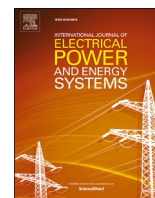
To cite this publication, please use the final published version (if applicable).
Please check the document version above.

Copyright

Other than for strictly personal use, it is not permitted to download, forward or distribute the text or part of it, without the consent of the author(s) and/or copyright holder(s), unless the work is under an open content license such as Creative Commons.

Takedown policy

Please contact us and provide details if you believe this document breaches copyrights.
We will remove access to the work immediately and investigate your claim.



Voltage vulnerability curves: Data-driven dynamic security assessment of voltage stability and system strength in modern power systems

Aleksandar Boričić^{a,b,*}, Marjan Popov^a

^a Delft University of Technology, Faculty of EEMCS, Mekelweg 4, Delft 2628 CD, the Netherlands

^b TenneT TSO, Utrechtseweg 310, 6812 AR Arnhem, the Netherlands

ARTICLE INFO

Keywords:

Power systems
System strength
Voltage stability
Data-driven
Resilience
Vulnerability
Dynamic security

ABSTRACT

Power systems evolve towards more renewable and less conventional electricity supply. This, however, brings significant technical challenges, as conventional sources naturally provide system resilience. One of the key dimensions of this resilience is system strength, which is rapidly depleted with the phase-out of fossil-based synchronous generation. This paper commences by exploring the intricate steady- and dynamic-state aspects of system strength, and consequently elevated risks of voltage instability. A new holistic definition of system strength is further proposed. Considering the stability challenges of modern power systems, grid operators need to be aware of any vulnerable grid sections and dangerous operating scenarios to always ensure system security and stability. Nevertheless, the rising complexity of modelling and analysis of dynamics in modern power systems makes this task increasingly challenging. The large number of grid locations with complex inverter-based generation and load, paired with parameter uncertainty, make deterministic analytical analyses of voltage stability and system strength increasingly challenging and time-consuming. A novel data-driven voltage stability and system strength assessment method, termed Voltage Vulnerability Curves (VVCs), is hereby proposed to address these challenges. The method is designed to cut through the complexity of modern power systems' dynamics and provide advanced system strength and voltage vulnerability insights.

1. Introduction

Renewable energy sources (RES) are the key solution for decarbonization of the energy sector [1]. However, due to their variable nature and fundamentally different technology compared to the conventional generation, power electronics are used to integrate RES into a power system [2]. RES are, therefore, often referred to as Inverter-Based Resources (IBRs), a term that encompasses wind generation, solar PV farms, batteries, HVDC connections, FACTS devices, and many types of loads. These resources typically operate in Grid-Following (GFL) mode, while replacing synchronous generators. The result is a natural degradation of inertia and system strength in power systems, which leads to many challenges in maintaining grid stability and dynamic security [3,4]. Some of these challenges are discussed in this paper in depth, especially related to system strength and voltage stability.

To deal with system stability challenges, Transmission System Operators (TSOs) use various tools in planning and operational timeframes to predict and analyze dangerous grid situations. One of the core tools and processes in this regard is the Dynamic Security Assessment (DSA), a

model-based approach where numerous dynamic time-domain simulations are performed continuously [5]. DSA can be implemented in many timeframes, covering aspects such as outage planning, operational planning, real-time operations, and look-ahead analysis. A high number of grid scenarios are simulated every day across hundreds or even thousands of credible contingencies, in an attempt to locate vulnerable grid sections and ensure dynamic security. This is commonly done in a very deterministic way, with fixed model parameters and credible disturbances. If insecurities are observed, appropriate mitigation actions can be taken to bring the system to a more secure operating state.

However, modern power systems experience a high dose of uncertainty. What used to be a single synchronous generator, with known fixed parameters and physics-driven behavior, is often replaced by many IBRs with dozens of parameters and states. These IBRs are seldom easy to model accurately, due to their sheer number as well as data limitations in terms of quality or proprietary characteristics. Furthermore, RES are also installed in distribution systems, known as Distributed Energy Resources (DERs), complicating the accurate modelling efforts further. Additionally, system demand is changing, where dynamic and inverter-

* Corresponding author at: Delft University of Technology, Faculty of EEMCS, Mekelweg 4, Delft 2628 CD, The Netherlands.

E-mail address: a.boricic@tudelft.nl (A. Boričić).

<https://doi.org/10.1016/j.ijepes.2025.110636>

Received 11 July 2024; Received in revised form 6 January 2025; Accepted 25 March 2025

Available online 17 April 2025

0142-0615/© 2025 The Authors. Published by Elsevier Ltd. This is an open access article under the CC BY license (<http://creativecommons.org/licenses/by/4.0/>).

based loads introduce intricate dynamic responses that are difficult to model, yet may play a large role in the overall grid stability [6–8]. All these trends result in a reduced efficacy of deterministic analytical methods, and the need to move to more stochastic, risk-based, and ultimately data-driven approaches to safely operate the systems of the future.

Moreover, it is becoming clear that RMS simulations cannot fully capture all dimensions of electromagnetic dynamics in modern IBR-rich grids [9–11]. The need for more accurate EMT simulations is rising. However, EMT has notably higher modelling requirements and much slower simulations' execution time. This is a major challenge for TSOs' operational tools such as DSA, where numerous scenarios across a broad network need to be analyzed quickly. It is therefore crucial to extract the maximum information possible out of RMS simulations, so EMT is used efficiently on a very limited and targeted number of cases only [12,13]. This is the premise of vulnerability assessment, to reduce the problem scale by detecting dangerous grid scenarios and weakest grid locations that may require deeper analysis or outright mitigation. Such an assessment becomes more relevant with the rising uncertainty and complexity in IBR-rich power systems [14].

The main contributions of this paper can be divided into two parts. The first part demonstrates theoretically and analytically how voltage stability and system strength evolve in modern power systems. A new holistic definition of system strength is introduced, and its classification and implications for power systems stability are discussed.

This is a basis for the second part, where Voltage Vulnerability Curves (VVC) method is introduced. The method is designed to numerically evaluate dynamic aspects of system strength and voltage stability, providing advanced grid security and vulnerability insights to grid operators. Several illustrative simulations are shown, demonstrating the efficacy of the new method. Finally, the impacts of uncertainty are embedded in the VVC method, further enabling the necessary probabilistic approach.

Both parts are novel and timely, as current understanding and estimation of system strength lags behind the observed necessity in grids with large RES penetration.

The paper is organized into six main sections. Section 1 introduces the challenges and the research motivation. In Section 2, an extensive technical discussion on voltage stability and system strength is presented, alongside the current scientific extent and novel insights relevant to the scope of this paper. Section 3 introduces the new evaluation method for voltage vulnerability and dynamic system strength. Section 4 presents simulation results and related discussion. In Section 5, the method is expanded to consider parameter uncertainty impacts. Finally, Section 6 concludes the paper and provides further research opportunities.

2. Voltage stability and system strength of modern power systems

This section explores various intricate aspects of voltage stability and system strength in modern power systems. The theoretical discussion and a newly proposed definition of system strength are accompanied by relevant analytical derivations and numerical simulations.

2.1. Voltage stability background

Power system stability is evolving together with the systems. The widely accepted classification is proposed in [15]. One of the important sub-types of modern power systems' stability is voltage stability.

Voltage stability is described as the ability of a system to maintain steady voltages at all buses while being able to deliver the power required by loads [16,17]. It concerns both small and large disturbances over the short- or long-term. This is shown in Fig. 1. Reactive power coordination across different time scales is central to maintaining stable voltages, particularly in transmission systems.

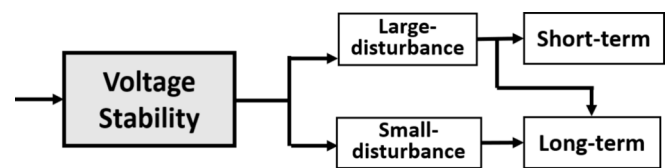


Fig. 1. Common classification of voltage stability.

A system is considered voltage secure if it can maintain stable voltages following credible contingencies or load changes. Expanding on this further, a system is considered voltage resilient (vulnerable) if it exhibits a relatively low (high) risk of cascading faults and voltage instability and collapse [14]. Observing the systems worldwide, voltage vulnerability has been increasing over the past decades, with voltage stability concerns rising [18]. This is seen in both long-term (static) voltage stability, related to steady-state maximum power transfer, as well as in large-disturbance short-term voltage stability. A much more comprehensive discussion on voltage stability and its sub-types is hereby omitted for brevity and can be found in [19].

For the focus of this paper, short-term voltage stability (STVS) is of particularly high importance. STVS considers dynamics of fast-acting demand such as induction motors, electronically controlled loads, and more recently, HVDC links, IBRs, and distributed energy resources (DERs) [19–21]. STVS is, therefore, more likely to be an issue in grid sections with more of these elements present, with the grid pushed to its limits [8]. Additionally, as IBRs directly rely on strong system voltages, severe voltage deviations and delayed voltage recovery pose a significant risk for cascading and consequent voltage stability. To appropriately analyze and simulate conditions that lead to STVS dynamics, a detailed representation of dynamic loads and nearby IBRs is necessary. Furthermore, STVS is negatively affected by the reduction of system strength, particularly of its dynamic component [14].

This profound relationship between voltage stability and system strength is central to this paper and is therefore discussed further from a technical perspective.

2.2. System Strength: Definition and classification

System strength has become one of the key concepts in modern power systems as the phase-out of fossil-based synchronous generation advances further. Grids or grid sections are more frequently referred to as weak, especially in (electrically) remote locations without synchronous generation proximity. Conversely, due to weather conditions and land availability, such remote grid locations are often very compelling for renewable generation. This makes grid strength evaluation crucial to ensure secure system operation and avoid system instabilities. However, as more renewable generation is integrated into power systems through power-electronics converters, the system strength concept of conventional power systems must also evolve, as it is becoming less applicable and inaccurate in modern IBR-rich power systems.

Various definitions of system strength are available in the literature. In conventional power systems, it was a synonym for short-circuit power (S_{sc}). Presently, the commonly used definitions express system strength as the sensitivity of voltage to variations in the current injection [22]. In other words, system strength is understood as voltage stiffness [23], analogous to inertia and frequency deviations relation. Others define system strength as a broader term comprising both inertia and voltage stiffness [24]. Additionally, system strength is discussed both in terms of steady-state operation [25] as well as in the dynamic state as the size of the voltage change following a disturbance [26]. Such a wide dispersion of definitions indicates that classification and understanding of system strength are still maturing. In an attempt to accurately and concisely reflect all relevant stability dimensions of system strength, a new holistic definition is proposed as follows:

System strength refers to the ability of a power system to maintain stable

voltages in steady- and dynamic-state and avoid related instabilities and cascading. Symptoms of low system strength include reduced voltage stability limits and maximum power transfer, higher voltage sensitivity, and elevated susceptibility to converter-driven interactions, oscillations, desynchronization, and instabilities.

It is important to highlight that besides the defined aspects, low system strength also introduces challenges for power system protection due to lower and non-conventional fault currents [27,28]. Moreover, lower system strength is known to result in amplified and more widespread voltage dips and transient overvoltages, increased harmonic distortions, flickers, and other power quality aspects [26,29]. The aspects of power quality and protection are not directly related to system stability and vulnerability and are therefore out of the scope of the discussion in this paper.

System strength can be also classified in a similar way as voltage stability, with steady-state (small-disturbance) and dynamic-state (large-disturbance) aspects (Fig. 2).

This differentiation is necessary for modern power systems due to the high non-linearity of IBRs and their very different behavior in steady- and dynamic-state. A modern power system could exhibit strong steady-state behavior, but simultaneously be very vulnerable to large disturbances (or vice versa). Readers are referred to a deeper discussion on this classification as proposed in [30,31].

Steady-state system strength aspects receive a lot of research and industry attention. Short-circuit capacity (S_{sc}) used to be the most common metric to describe system strength [32]. To understand S_{sc} and its relation to system strength in conventional and modern power systems, a simple but illustrative system in Fig. 3 is hereby used [33].

The system depicts a source (in this case an IBR) connected to the bus i , while a Thevenin source represents the rest of the power system. The voltage at the point of the IBR connection can be expressed as a function of Thevenin's voltage and voltage drop across the impedance.

$$\underline{V}_i = \underline{V}_s - \underline{Z}\underline{I}_i \quad (1)$$

For a small change in IBR's current $\Delta \underline{I}_i$, the consequent change in voltage can be calculated as follows:

$$\underline{V}_i + \Delta \underline{V}_i = \underline{V}_s - \underline{Z}(\underline{I}_i + \Delta \underline{I}_i) \quad (2)$$

$$\Delta \underline{V}_i = -\underline{Z}\Delta \underline{I}_i \rightarrow \underline{Z} = -\frac{\Delta \underline{V}_i}{\Delta \underline{I}_i} \quad (3)$$

From Eq. (3), Thevenin's impedance is directly linked to the relative change of voltage per change of current, which is often described as *voltage sensitivity*. Voltage sensitivity provides information on system strength; when $\Delta V/\Delta I$ is high, it means that the bus voltage is very sensitive (susceptible) to the changes in infeed current (power), often called a "weak bus". In other words, the current (power) injected by the IBR in Fig. 3 will have a big impact on the bus voltage \underline{V}_i . If this is not the case, the grid voltage can be described as strong or stiff. Voltage sensitivity can be further expressed from the perspective of S_{sc} , as shown in

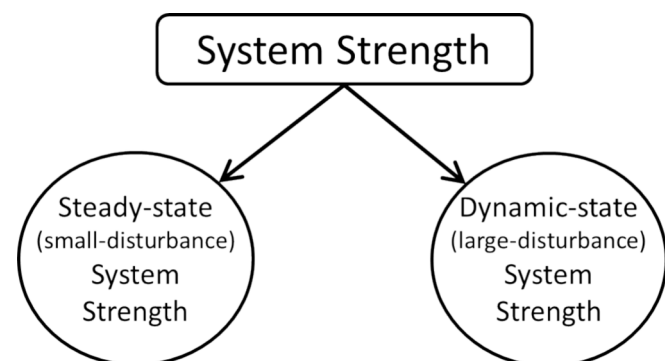


Fig. 2. Latest classification of system strength in modern systems.

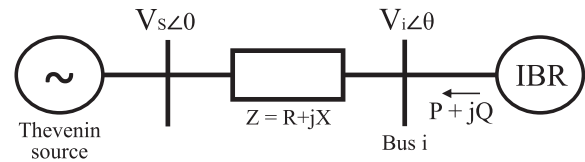


Fig. 3. IBR connected to a grid represented by Thevenin's source.

equations (4) and (5), where I_{sc_i} is the short-circuit current that would flow through the bus in the case of a zero-impedance three-phase short-circuit fault.

$$S_{sc_i} = \underline{V}_i I_{sc_i} = \frac{V_i^2}{\underline{Z}} \quad (4)$$

$$S_{sc_i} \approx \frac{1}{\underline{Z}} \approx \frac{\Delta \underline{I}_i}{\Delta \underline{V}_i} \quad (5)$$

These two expressions reveal a very clear relationship between S_{sc_i} , voltage sensitivity, and consequently system strength. Eq. (5) depicts the inverse (direct) proportionality between S_{sc} and voltage sensitivity (system strength), and the inverse proportionality between Thevenin's impedance and S_{sc} and system strength. Therefore, buses with relatively high (low) S_{sc} are generally called strong (weak) buses. However, this needs to be put into perspective relative to the size of the connected generating unit (e.g., IBR in Fig. 3). For this purpose, various ratios are defined in the industry and academia, such as Short-Circuit Ratio (SCR), Weighted Short-Circuit Ratio (WSCR), Equivalent Short-Circuit Ratio (ESCR), Excess System Strength (ESS), and many more. A comprehensive review and analysis of the most common system strength metrics can be found in [14,30–34] and is hereby omitted for brevity.

What all these metrics have in common is that they assume a linear system around its operating point. In other words, they only evaluate the *steady-state system strength*, and do not consider the intricate aspects of *dynamic-state system strength*, as shown in Fig. 2. and discussed in detail in [14,30]. This shortcoming will be further demonstrated with illustrative numerical simulations.

2.3. Relationship between system strength and voltage deviations: Numerical examples

To be able to simulate complex voltage deviations and instabilities that may occur in modern power systems, it is necessary to employ advanced simulation models. For this purpose, the IEEE Test System for Voltage Stability Analysis and Security Assessment is hereby used [35]. This test system is based on the Nordic Grid and can replicate various dynamics relevant to voltage stability evaluation. The single-line diagram of the model is shown in Fig. 4.

To illustrate the relationship between short-circuit power and voltage deviations, S_{sc} of 130 kV busbars is calculated in DIGSILENT PowerFactory based on the IEC 60909–2016 standard. The results are depicted in Fig. 5.

There is a large variation in S_{sc} across the system. This is a consequence of several factors: proximity to synchronous generators, impedances of the lines, how meshed the nearby grid is, etc. To illustrate how S_{sc} relates to voltage dips, a 3-phase short-circuit is applied to each bus, and the voltage response is measured. Fault resistance of 2.5 Ω is used for each simulation. The results are plotted in Fig. 6, with a color bar label representing S_{sc} of the respective busbar, as per Fig. 5. Voltage dip ΔU_f is measured as the difference between the pre-fault voltage and the voltage nadir during the fault.

From Fig. 6, it can be seen that S_{sc} and voltage dips are very much inversely related. Busbars with a higher (lower) S_{sc} generally experience a lower (higher) fault-induced voltage dip. This is essentially the primary reason why S_{sc} is often used as a proxy for system strength in terms of voltage sensitivity. Buses with higher (lower) S_{sc} will therefore have

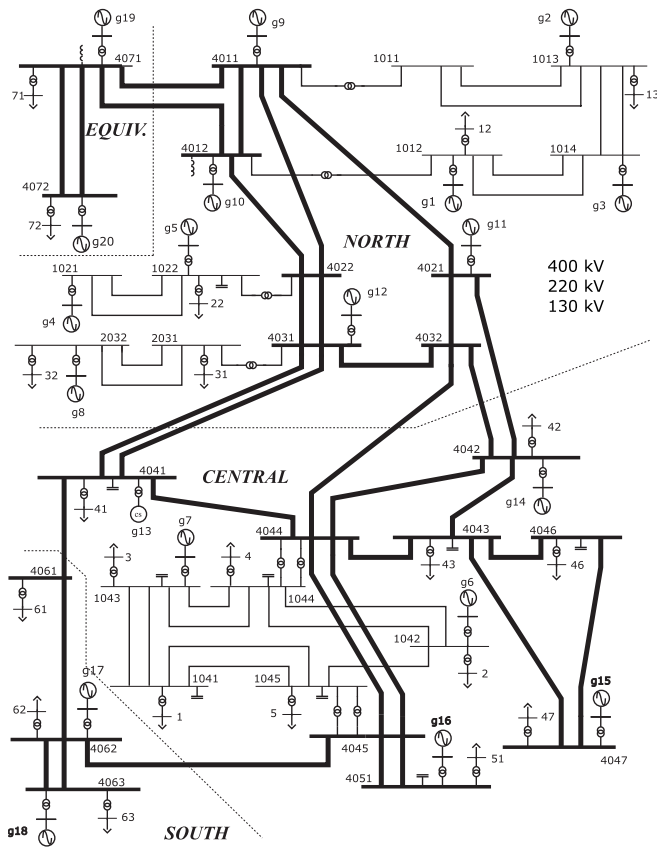


Fig. 4. IEEE Test System for Voltage Stability Analysis and Security Assessment.

lower (higher) voltage sensitivity, as analytically demonstrated in equations (1) to (5).

However, this analysis has a couple of assumptions and simplifications. The first one is that the system can be replicated with a Thevenin equivalence. For power systems with an increasing share of IBRs, this

assumption becomes less accurate due to control-driven non-linearities. The other important assumption is that the demand is static and passive. As such, these loads do not have a major impact on fault and post-fault voltage dynamics. While this was a reasonable assumption in conventional power systems, it has become progressively less accurate in modern power systems. The first reason for this inaccuracy is the increasing penetration of DERs in the medium- and low-voltage networks. What used to be a passive distribution network (PDN) is nowadays much more often an active distribution network (ADN), with bidirectional power flows.

Furthermore, the second reason is that dynamic loads become more common in distribution systems, as electrification takes place in sectors previously run on fossil fuels, like heating, transportation, industrial processes, etc. Therefore, the composition of ADN may play a major role in grid dynamics and can be particularly relevant when short-term voltage deviations and stability are concerned. The proliferation of RES and the transition from PDN to ADN is therefore invalidating the assumption that S_{sc} can be directly related to system strength.

Lastly, voltage dynamics with RES and ADN occur not only during the fault period but also in the seconds after the fault, known as the post-fault dynamics. Therefore, to capture the full scope of voltage deviations related to dynamic system strength, evaluating only the voltage dip during the fault is insufficient. The entire short-term response needs to be captured and evaluated instead.

To analyze these aspects and relate them to the dynamic-state system strength, this paper proposes a novel data-driven method, introduced in the following section.

3. Methodology: Voltage vulnerability curves

The dynamic impact of load and DER response on grid resilience was shown to be very important to consider when analyzing grid stability and strength [8,36]. However, system strength, as one of the main aspects of grid resilience and vulnerability, is typically evaluated only from the steady state perspective, as described in [14,30]. This evaluation, while important for the steady-state operation, completely misses the intricate dynamical response of dynamic loads and DER and their impact on dynamic state system strength.

To capture the dynamic aspects that are often very complex and

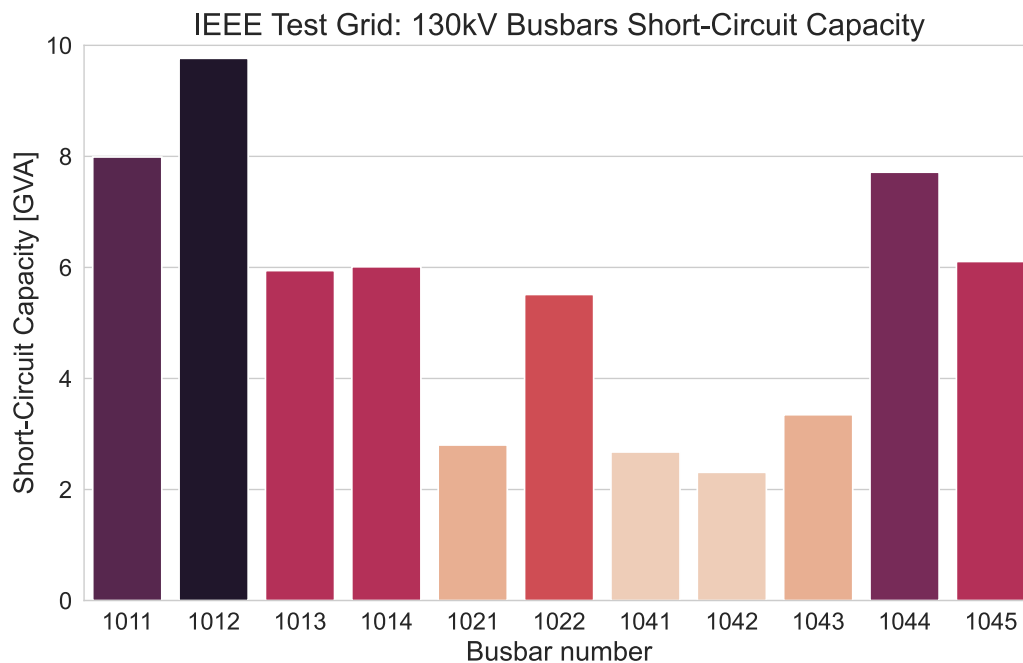


Fig. 5. Short-circuit capacity of every 130 kV busbar in the IEEE test system based on the IEC 60909–2016 standard.

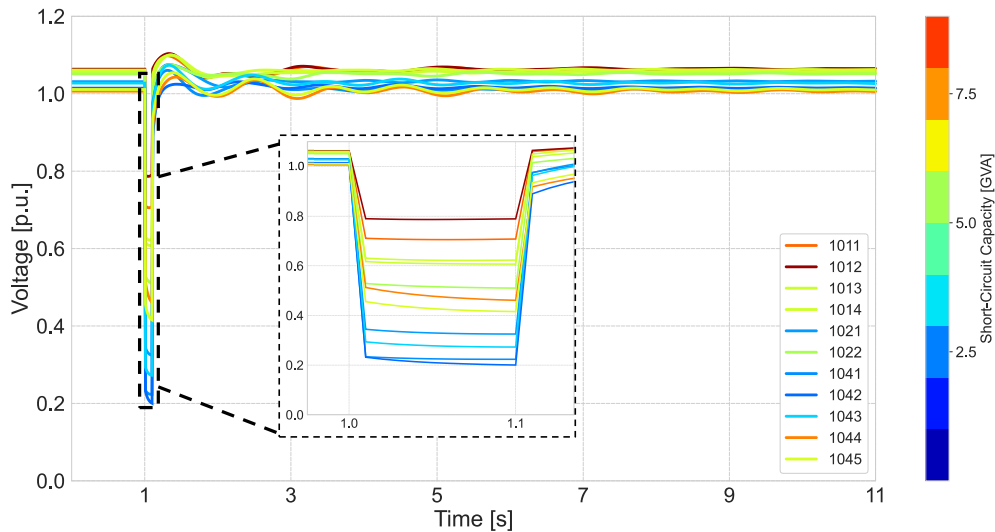


Fig. 6. Dynamic simulations illustrating the inverse relation between voltage drop (ΔU_f) and short-circuit capacity of a bus.

consist of many discrete control actions, time-domain simulations are often necessary. Additionally, the challenge for grid operators is further emphasized by the large number of IBRs and their controls that need to be represented by a careful combination of detailed and generic models. Moreover, the results of such simulations are dependent on the initial conditions, i.e. the operating scenarios, putting further stress on computational demand.

Nevertheless, computational capabilities have improved significantly over the past years, primarily thanks to cloud computing, parallelization, and task automation. Scripting and parallelization offer the possibility to rapidly and efficiently automate numerous time-domain simulations across a wide range of operating scenarios and parameters, spreading the computational tasks efficiently. Inside modern TSOs, this has already become a common practice, where hundreds of credible contingencies are simulated for operational planning and in real time. This all takes place in RMS time-domain tools, often in just a matter of minutes. Such approaches are widely used in modern DSA tools, as hereby exemplified to demonstrate the newly introduced method. This is illustrated in Fig. 7.

However, while computational demand can be managed through automation and parallelization, the big data sets originating from such an approach are very time-consuming to analyze. Power system software typically only provide binary stability information. It is therefore also necessary to have a scalable and fast data-driven approach that can quantify the severity of results, such as voltage deviations,

automatically. This information can be thought of as an automatic severity and risk assessment of a wide range of scenarios and contingencies, giving the operator much broader insight into the dynamic system state.

3.1. Cumulative voltage deviation method

To capture the full scope of fault and post-fault voltage deviations, a new method is developed and introduced in [37,38], Cumulative Voltage Deviation (CVD). CVD is derived based on Eq. (6–8) and is graphically depicted in Fig. 8.

$$V_U(t) = (1 + a)V_0 - t/b \quad (6)$$

$$V_D(t) = (1 - a)V_0 + t/b \quad (7)$$

$$CVD = \sum_{t=t_f}^{t=t_f+T} \begin{cases} V(t) - V_U(t), & \text{if } V(t) > V_U(t) \\ V_D(t) - V(t), & \text{if } V(t) < V_D(t) \\ 0, & \text{else} \end{cases} \quad (8)$$

In Eq. (8), t_f is the fault inception time, and T is the evaluation time window. $V_U(t)$ is the upper threshold (blue dashed line in the upper graph in Fig. 8), whereas $V_D(t)$ is the lower threshold (the orange dashed line). Eq. (6) and (7) define the envelope of permissible voltage levels. The parameters a and b define initial points (A and C in Fig. 8), and the final points (B and D in Fig. 8), including thresholds of $V_U(t)$ and $V_D(t)$.

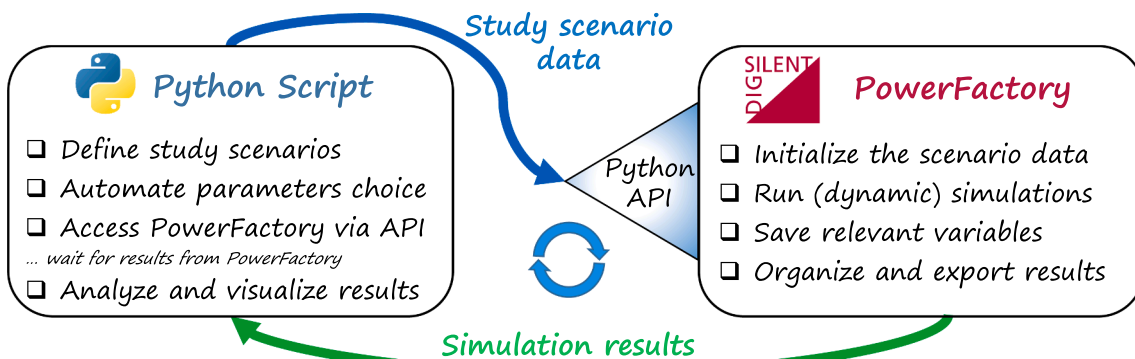


Fig. 7. Automation framework utilizing Python scripting and DigSILENT PowerFactory dynamic simulations used in this paper.

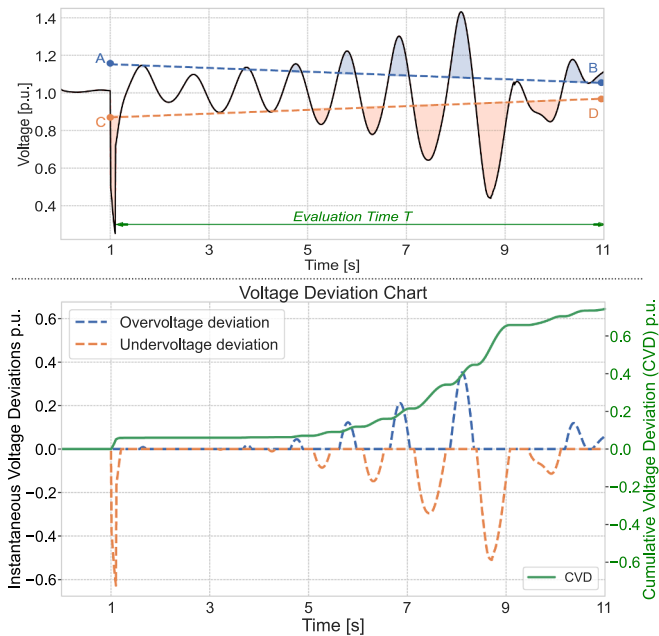


Fig. 8. Visualization of the CVD method for an illustrative case of oscillatory voltage deviations.

To detect and quantify severe voltage deviations, values $a = 0.15$ and $b = 100$ are utilized. From a practical point of view, this means that the evaluation starts when the voltage overshoots point A or C, i.e. $\pm 15\%$ from the pre-fault voltage, moving towards $\pm 5\%$, as per common thresholds for large voltage disturbances and recovery values. This is elaborated on and tested further in [37].

The CVD method is a data-driven approach that applies a linear envelope to quantify the severity of voltage deviations following a disturbance. Further description of the methodology and its extensive testing and suitability in evaluating voltage deviations is shown extensively in [37].

Based on simulations shown in Fig. 6, fault-induced voltage drop ΔU_f is calculated and plotted against S_{sc} for each respective busbar.

Furthermore, CVD is also calculated for each busbar and hereby plotted. Each simulation is shown with a dot in the scatterplot, further regressed with a simple linear regression model to visualize the inverse relationship. The results are shown in Fig. 9.

What is observed from Fig. 9 is that both ΔU_f and CVD have a strong inverse linear relationship with S_{sc} . This is expected, as per Section 2, and both metrics can quantify voltage deviations in an intuitive way. Therefore, even simple methods such as S_{sc} can be successfully used to quantify system strength in relatively linear conventional power systems with passive distribution systems.

In the next two sections, the assumptions of static load and conventional generation will be relaxed in order to show how S_{sc} and ΔU_f become progressively less relevant as system strength indicators of modern power systems.

3.2. Voltage Vulnerability Curves (VVC)

A new method is developed and proposed here, termed Voltage Vulnerability Curves (VVCs). The method expands on the CVD algorithm to provide insights into dynamic state system strength. It is exemplified and described in Fig. 10.

The right part of Fig. 10 shows an example of a VVC plot. The Y-axis indicates the severity quantification of a voltage disturbance in kV-sec or per-unit-sec, relying on the already-introduced CVD method [37]. The X-axis depicts the increasing duration of the fault in (milli)seconds. As per the algorithm shown on the left of Fig. 10, a series of dynamic simulations are performed, where Δt_f is increased in steps until a pre-defined t_{max} value. This value can be chosen as a maximum expected total fault-clearing time, based on protection coordination. This should include not only relay operation but also typical circuit breaker (CB) operation time and arc quenching [39]. It may also include N-1 (N-2) protection or CB malfunction assumptions.

The resulting CVD values are collected for several discrete simulation scenarios and are scatter-plotted on the VVC plot on the right of Fig. 10 (black circles). These circles therefore depict simulation-based CVD values for their respective Δt_f . Once all the simulations are completed, an interpolated curve is created, depicted in blue in this example. Interpolation is a method of constructing new data points based on the range of a discrete set of known data points. The way to perform the interpolation will be discussed later in this paper.

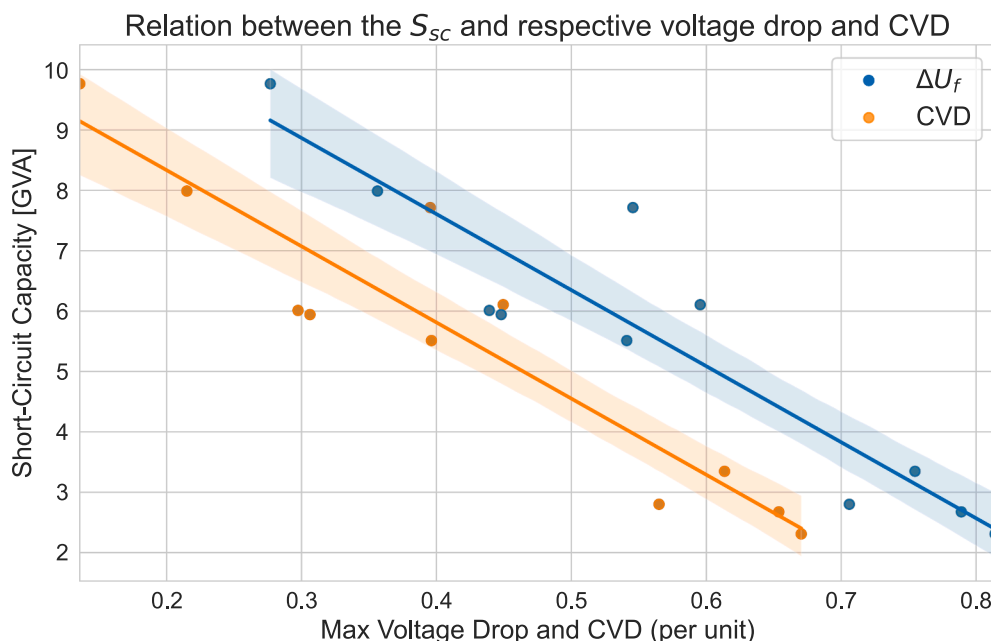


Fig. 9. Relationship between S_{sc} and voltage deviations measured by voltage drop ΔU_f and CVD, for each 130 kV bus in the system.

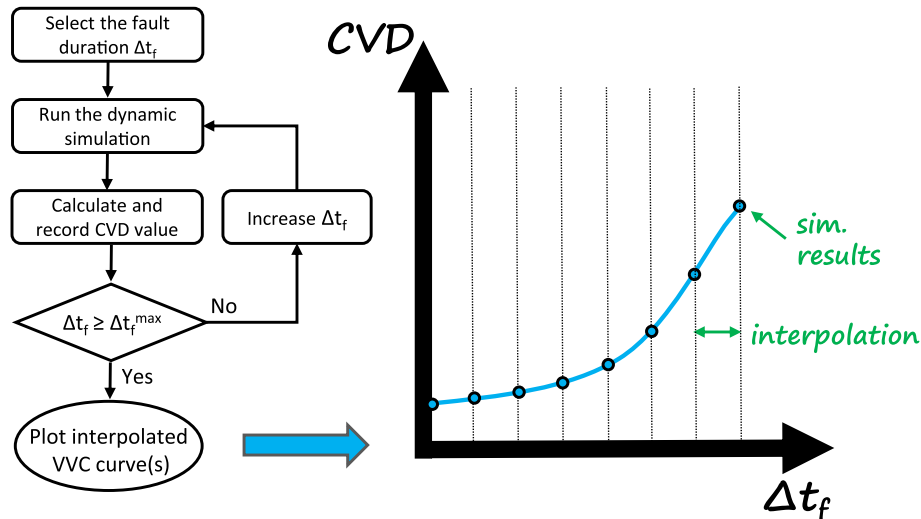


Fig. 10. The methodology of the VVC method (left) and the example of the resulting VVC plot and curve (right).

The created VVC curve can be understood as follows. For a certain simulation scenario, the CVD value is calculated, indicating the severity of a disturbance for the given conditions. This severity will primarily depend on two aspects: the system’s strength and fault duration. However, this severity will also depend on the composition of load and (distributed) generation and their non-linear contribution to voltage dynamics [8]. Ultimately, the higher the voltage deviation, the weaker the system, resulting in elevated cascading and voltage instability risks. Therefore, VVC is not meant to classify a scenario in a binary manner (stable or not), but rather provide a data-driven risk-based approach more suitable for weak systems with high uncertainty. The scenarios that exhibit the most vulnerability can then be avoided or mitigated in operational planning, and the weakest buses can be strengthened with long-term grid expansion planning. Alternatively, additional detailed and targeted studies, such as EMT, can be performed if needed.

The core idea of the methodology is a relative strength comparison, to pinpoint the weakest buses in the grid for the respective operating scenario. This is most efficiently done in operational planning or longer-term grid expansion planning, where sufficient time for such analysis is available. Additionally, engineering judgement can be used to limit the number of scenarios and buses of interest, for instance by focusing on more remote (less meshed) grid areas, and areas with dominant inverter-based generation.

CVD and VVC are purely data-driven methods and there is no deterministic theoretical instability threshold that can be applied across different systems. Nevertheless, a pragmatic weakness threshold is hereby proposed based on Low Voltage Ride-Through (LVRT) requirements. Such a threshold is in line with common practice, as LVRT requirements are commonly used to determine voltage security violations within DSA applications. The general LVRT requirements in the EU are defined by Entso-e Requirements for Generations (RfG) [40,41]. This

is illustrated in Fig. 11. The LVRT curve for power park modules in RfG is shown, with the most stringent limitation.

The encompassed area of the voltage-duration curve (color-marked in Fig. 11) is calculated, resulting in a value of 1.3 per-unit-sec. This value is hereby proposed as the weakness threshold for CVD and respective VVC methods. The rationale for this lies in the fact that if CVD of a particular bus has breached this value, the voltage experiences a significant post-fault deviation, and the LVRT conditions are likely not met. This results in a high risk of IBRs and DERs disconnections and an increased danger of cascading and voltage instability. In other words, the grid location can be considered weak from the dynamic-state perspective, as discussed in Section 2.2.

This threshold is not always a direct indication of imminent voltage instability. Instead, it can be thought of as a quantitative evaluation, indicating that the bus voltage is dynamically weak with increased risks of instability. The threshold can be fine-tuned as per specific national grid codes, depending on the system being analyzed. Regardless of the threshold, the main goal of the analysis remains to locate the relatively weakest buses in the system, where a threshold value is not strictly necessary for effective results.

In the next section, the VVC efficacy in quantifying voltage deviations will be demonstrated. The previous assumptions of static load and conventional generation will be relaxed in order to show how S_{sc} and ΔU_f become progressively less accurate and relevant as dynamic state system strength indicators of a modern power system. Instead, the newly developed VVC method is benchmarked against S_{sc} , providing much broader insights about dynamic state system strength.

4. Simulations, results, and discussion

VVCs are hereby utilized to evaluate the dynamic system strength of buses with various DER and loads. The analysis commences with static loads, followed by an introduction of dynamic load models with delayed voltage recovery, and DERs with partial low-voltage tripping. Finally, in the last part of this section, the analysis will demonstrate the suitability of VVC for comparing the dynamic system strength of various buses in a power system.

4.1. Static load simulations with VVC

Initial simulations are performed on the system from Fig. 4. The demand is modelled as static, with original system parameters as per [42]. For each busbar, a VVC is created by a series of dynamic time-domain simulations in DIgSILENT PowerFactory with Python scripting

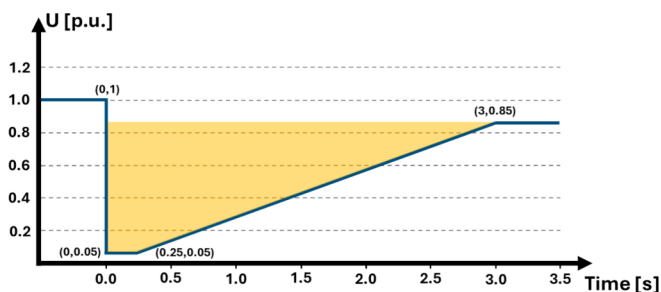


Fig. 11. Stringent LVRT curve from the Entso-e RfG network code.

(Fig. 7). In every consecutive simulation, fault duration is increased, alongside the severity of the disturbance, as described in Section 3. For each busbar, a voltage vulnerability curve is created by linearly interpolating the simulation results. Furthermore, the curves are color-coded to indicate how S_{sc} relates to the results. The VVCs are plotted in Fig. 12.

What can be seen from the results is that each VVC is linear. Furthermore, the color-coding shows that buses with larger S_{sc} experience lower voltage deviations. Therefore, for the case of static loads and conventional power systems, the VVC method leads to the same conclusions as simpler methods like S_{sc} . In other words, the conventional system response is linearly related to the disturbance severity, and one can often simply determine both steady- and dynamic-state system strength aspects from a single and easily computed indicator such as S_{sc} , without a need for more complex analytical or numerical analysis. However, the situation changes in modern grids, as further demonstrated.

4.2. Dynamic loads and delayed voltage recovery evaluation with VVC

In this subsection, the conventional power system in Fig. 4 is expanded to exemplify some of the modern aspects of loads. The static load at busbar 1041 is replaced with a WECC dynamic load with a large share of motor type D, i.e., single-phase A/C units [43]. This change is introduced to simulate the effects of stalling and Fault Induced Delayed Voltage Recovery (FIDVR). More details on this complex voltage mechanism can be found in [15,44,45].

A series of faults is simulated on busbar 1041 with increasing fault duration. Details of the utilized simulation parameters are listed in the appendix. The resulting voltages are plotted in Fig. 13 with green (red) color indicating the least (most) severe simulated scenario.

From Fig. 13, one can observe the occurrence of FIDVR events, with progressively deeper voltage sags. This is expected and in line with the understanding of FIDVR events [43–45]. The novelty here is how this effect is quantified. Voltage vulnerability curves are used, as described in Section 3. The VVCs corresponding to simulation results from Fig. 13 are plotted in Fig. 14.

A clear benefit of using VVCs over S_{sc} appears here. The green line

indicates the VVC of a system with static load only, as per Section 4.1. Meanwhile, the blue line indicates VVC for the case of dynamic load. For fault durations below 200 ms, there is almost no difference between the curves. In other words, for these cases, dynamic state system strength is comparable regardless of the load type. However, as fault severity increases due to larger fault duration, the curves start to diverge as FIDVR events unfold.

Events with a larger fault duration end up having much deeper and longer-lasting voltage deviations, indicating a dynamically vulnerable and weakened system. If S_{sc} was used as a system strength and voltage sensitivity metric, in this case, it would indicate the same value (severity) for both cases. Therefore, the bus strength would be significantly overestimated for longer fault durations with dynamic loads. Meanwhile, VVC demonstrates how larger fault duration, and therefore severity, affect the post-fault voltage response, providing new insights into dynamic grid security.

4.3. Distributed energy resources and low-voltage tripping with VVC

Active distribution systems often have a variety of DERs. These are located on low-voltage and/or medium-voltage levels. Depending on the voltage level and the DER nominal power, different low-voltage ride-through (LVRT) settings are applied, as per various grid codes [46]. In this paper, DER units are represented using the DER_A model [47–49], with more details listed in the appendix.

It is hereby demonstrated how partial LV-DER and MV-DER tripping could affect post-fault voltage response and stability. Simulations are performed with varying fault duration. As fault duration increases, LVRT implies that more DERs will disconnect, intentionally or not [46,50]. The voltage responses are shown in Fig. 15. Once again, the green (red) color indicates the least (most) severe case.

As seen in Fig. 15, post-fault voltage sag occurs due to the partial disconnection of DER resources. Furthermore, the last few simulations show an even larger voltage drop with a potential for voltage collapse. This occurs as MV-DER also disconnects for larger fault durations.

The corresponding VVC is plotted in Fig. 16. Furthermore, percentages in the plot indicate the LV-DER disconnections amount for each

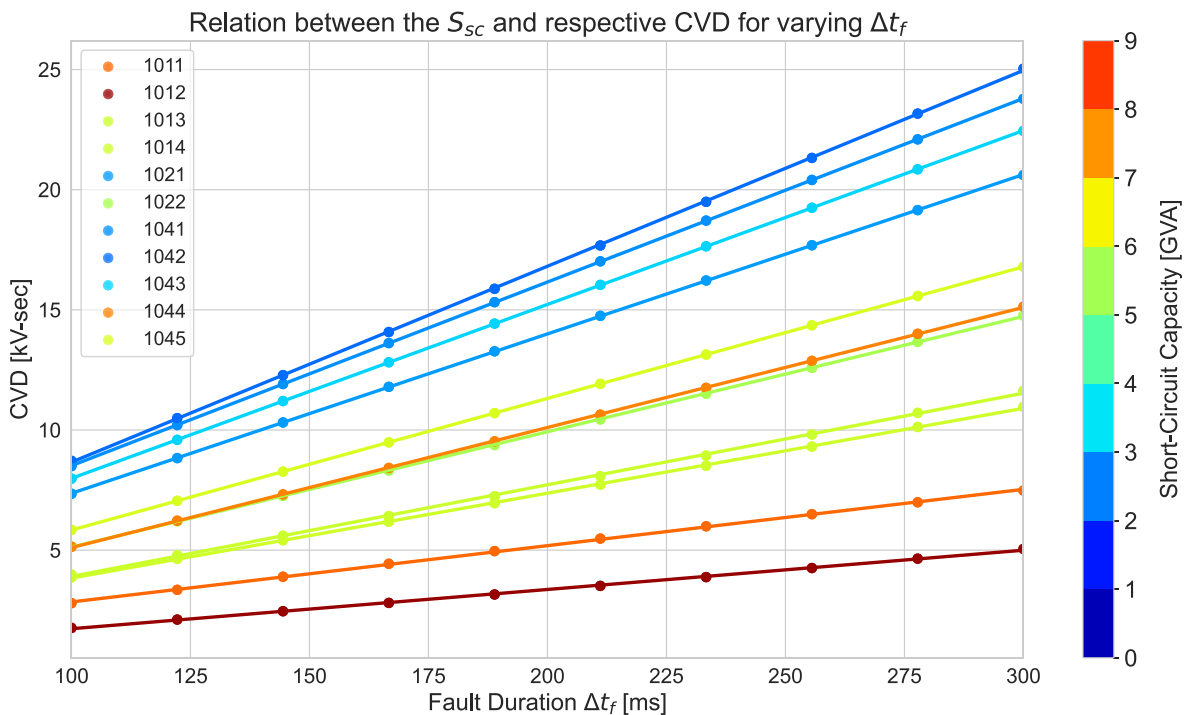


Fig. 12. Voltage vulnerability curves for 130 kV buses in the IEEE test system based on simulations from Section 3.

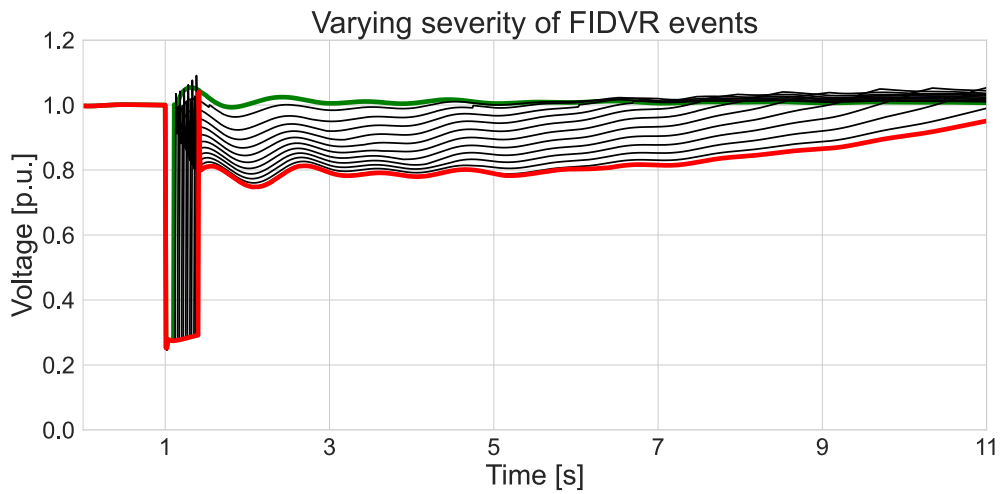


Fig. 13. Voltage responses of bus 1041 for a variety of scenarios.

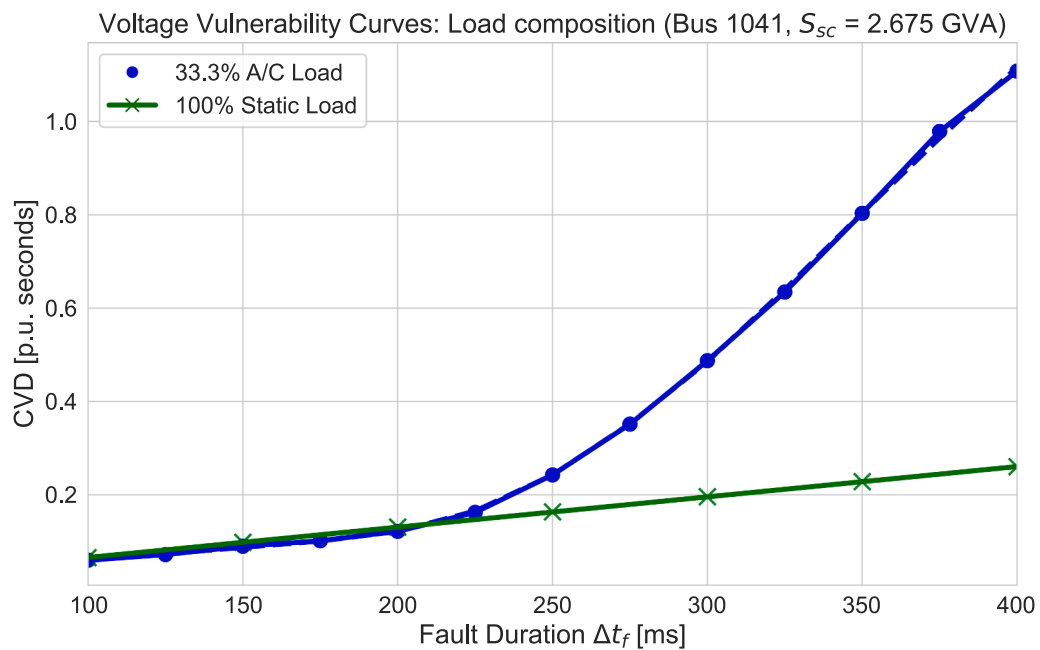


Fig. 14. Voltage Vulnerability Curves (VVC) for the case in Fig. 13. compared with a base case with only static load.

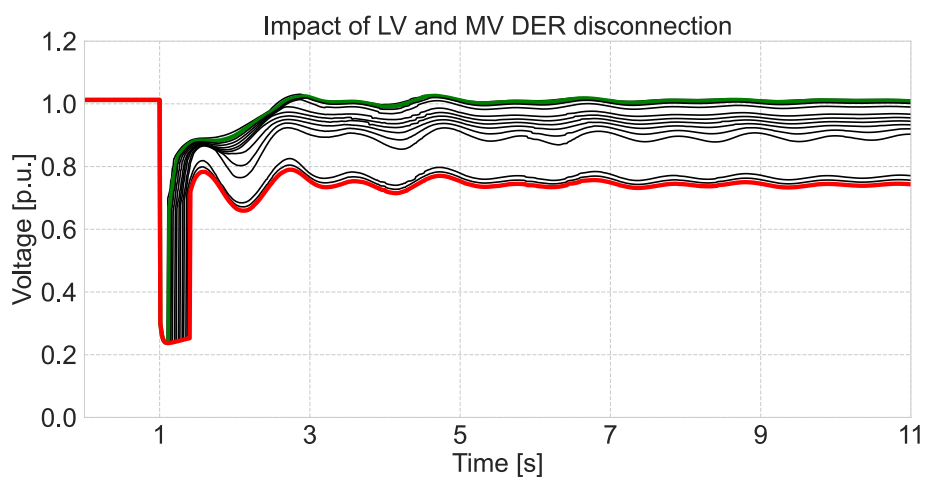


Fig. 15. Voltage response of bus 1041 with increasing fault duration which leads to partial DER disconnections.

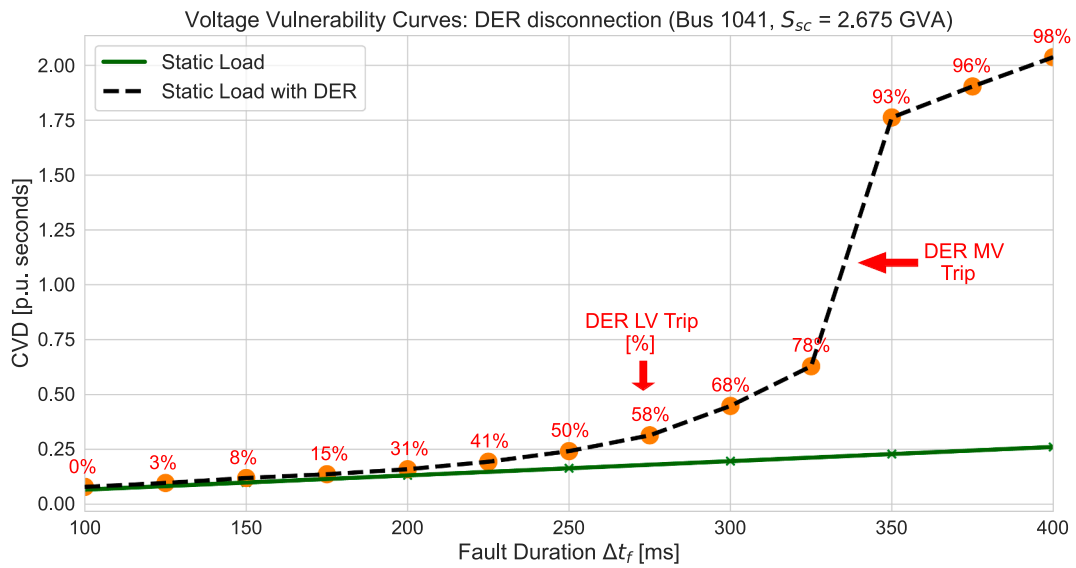


Fig. 16. Voltage Vulnerability Curves for the case in Fig. 15 compared with a base case with only static load.

simulation, as well as when the larger MV-DER unit tripped.

For short fault duration, the VVC with only static load is very similar to the VVC with DERs. In other words, the two systems are of comparable dynamic system strength. However, as the fault duration and severity increase, non-linearities appear as LV-DERs begin to partially trip, as indicated in the plot. Furthermore, for cases above 325 ms, MV-DER also trips, exposing the system to an even higher post-fault voltage drop with CVD beyond 1.3 per-unit-sec. For a very long fault duration, almost all LV-DERs and the MV-DER in this indicative example have

tripped, as per their illustrative LVRT settings listed in the appendix.

These simulations exemplify a few important points. Firstly, DERs can have a large impact on local post-fault voltage deviations and therefore system strength. This has been previously reported in the literature [8,36]. Secondly, if the system strength of such a busbar was evaluated using only S_{sc} , it would be severely overestimated. By using VVC, system operators can observe how partial and total disconnections of various DERs affect system response and obtain more information about the dynamic system strength of various buses given changing

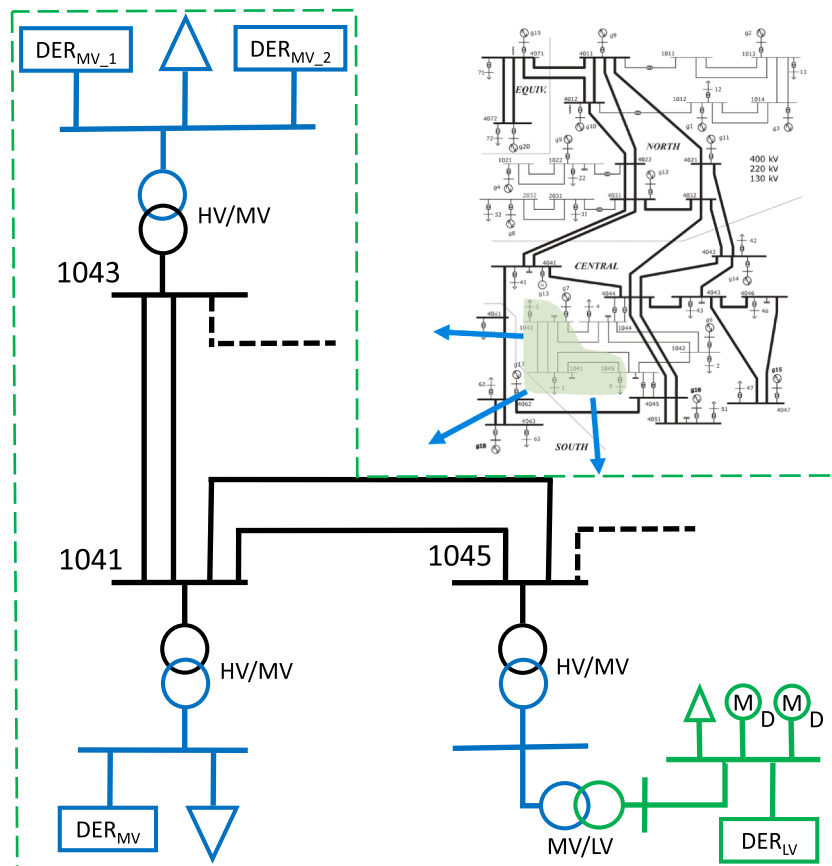


Fig. 17. Zoom-in on the altered section of the system, showing 130 kV buses (1041, 1043, 1045) with different demand compositions.

severity of faults.

4.4. Comparison of different distribution network compositions with VVC

In this subsection, the system from Fig. 4 is altered in a few ways. Loads of busbars 1041, 1043, and 1045 have been replaced from static loads to different compositions of dynamic loads with DER, as shown in Fig. 17. This change is implemented with the goal of demonstrating how a comparative analysis of dynamic system strength across different buses can be performed by using the newly proposed VVC methodology.

Similarly to previous analyses, simulations indicate the response of each busbar exposed to a 3-phase short-circuit with increasing fault duration. The results are plotted in Fig. 18 for each bus, respectively. Green (red) colors indicate the least (most) severe simulated scenarios.

The voltage responses of busbar 1041 are depicted in the uppermost plots of Fig. 18. One can note that bus 1041 has the lowest short-circuit capacity of the three, $S_{sc} = 2.67\text{GVA}$. As depicted in Fig. 17, bus 1041 contains a static load and a DER unit connected to the medium voltage level. When subjected to a fault, a voltage drop occurs, followed by an increasingly large post-fault voltage deviation. In the most severe case

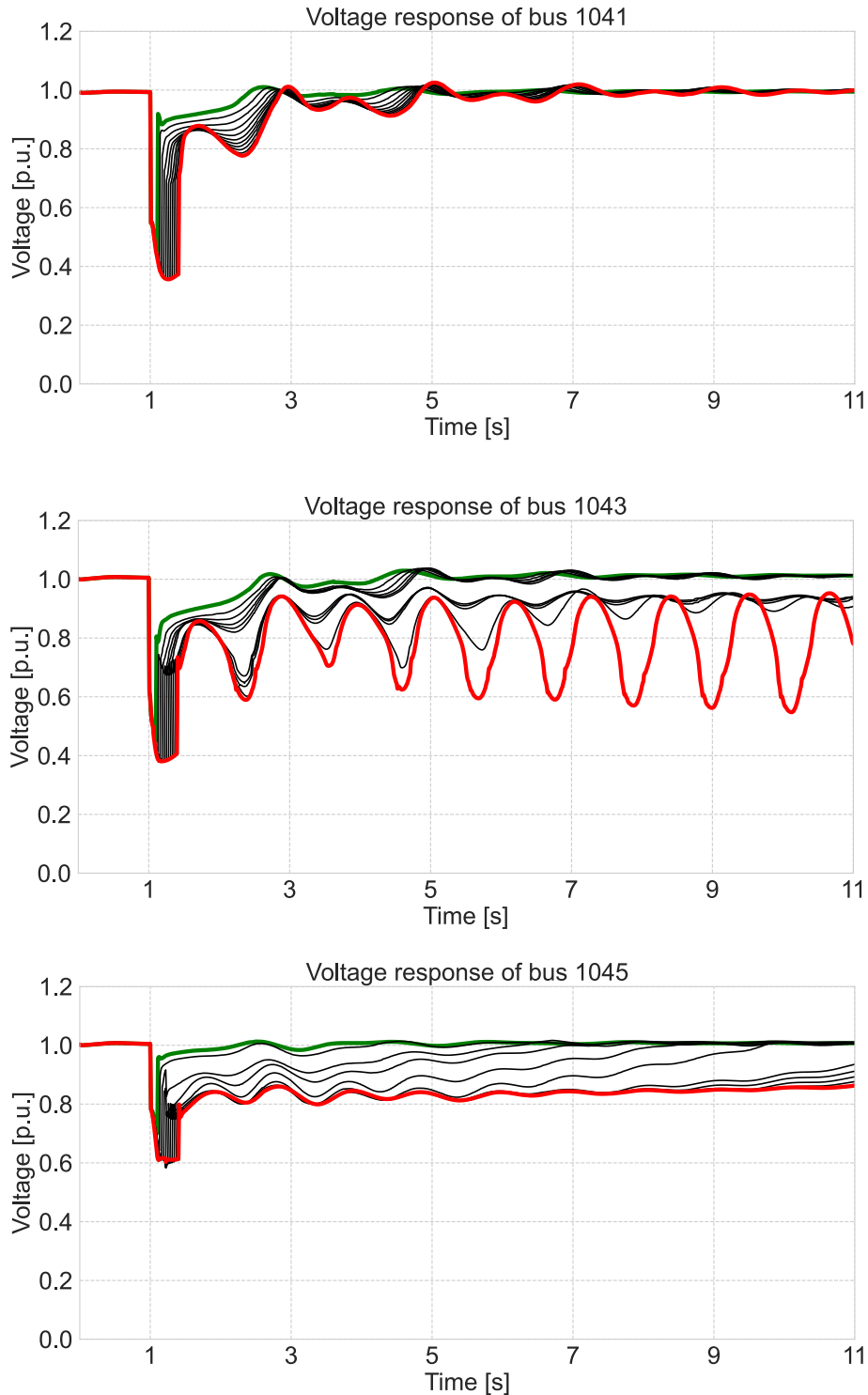


Fig. 18. Voltage responses of buses 1041 (top, $S_{sc} = 2.67\text{GVA}$), 1043 (middle, $S_{sc} = 3.34\text{GVA}$), and 1045 (bottom, $S_{sc} = 6.10\text{GVA}$) for a varying fault duration Δt_f .

(red), voltage experiences slight oscillations and delayed recovery, but manages to recover successfully without severe voltage deviations.

The voltage response of bus 1043 is depicted in the middle curves in Fig. 18. Bus 1043 has a somewhat higher short-circuit capacity than bus 1041, $S_{sc} = 3.34\text{GVA}$. Its demand composition is similar to the one of bus 1041, however, with two DER units connected to the MV grid. One of them is assumed to be able to withstand a low-voltage condition of up to 200 ms, while the other one up to 325 ms. As seen from the curves, voltage responses vary a lot as Δt_f increases. For the least severe fault duration, the response highlighted in green is similar to the one of bus 1041. However, as fault duration increases, voltage deviations intensify, eventually resulting in DER disconnections and severe voltage oscillations which would likely lead to short-term instability.

Finally, the voltage response of bus 1045 is shown in the lower plot of Fig. 18. Bus 1045 appears to be much stronger than the other two in terms of short-circuit capacity, with $S_{sc} = 6.10\text{GVA}$. This bus contains two dynamic loads of D-type, with one of them modelled as more prone to stalling.

Additionally, an aggregated LV-DER unit representing a large number of PV panels and/or other small generating units is connected. As fault duration increases, so does the amount of stalled dynamic load and partial LV-DER disconnections, resulting in post-fault low-voltage events.

Based on these voltage responses, respective voltage vulnerability curves are created as per the methodology in Section 3 and are plotted in Fig. 19. Several important insights are exemplified with this plot.

Firstly, note the difference in S_{sc} of each busbar, as depicted in the legend of Fig. 19. For faults with low duration (left part of the plot), S_{sc} is indeed correctly indicating that 1045 is the strongest bus, followed by 1043 and 1041 (blue, red, and green, respectively). However, as fault duration increases, things start to change quickly. Starting from ~ 200 ms fault duration, bus 1045 begins to experience FIDVR events, and quickly becomes effectively the weakest bus. Meanwhile, bus 1043 sees an increase in voltage deviations starting from 250 ms, as some of its LV-DER units begin to trip. Therefore, in the range of 200 to 350 ms fault duration, busbar 1045 is the weakest, while 1043 is the strongest bus. Note that this is completely opposite compared to what S_{sc} would indicate.

As fault duration increases towards 400 ms, bus 1043 starts experiencing severe voltage deviations and oscillations, as per the middle plot of Fig. 18. Therefore, its VVC rapidly shoots upwards, reaching around 1.5 per-unit-sec CVD value. Therefore, in the > 350 ms range, busbar

1043 is the weakest bus, followed by 1045 and finally 1041. Once again, S_{sc} would imply a completely different evaluation of system strength, which would not be accurate for such cases. In this sense, VVC is far superior in providing information about dynamic system strength and voltage sensitivity.

Based on the analysis in this section, it can be concluded that VVC provides much more information about system strength compared to S_{sc} . By directly and automatically evaluating voltage deviations, it is possible to obtain a much clearer picture of the dynamic-state system strength aspects of busbars of interest. This is particularly important for systems with larger penetration of IBRs and dynamic loads, where weak grid challenges become more emphasized [14].

The analysis was demonstrated on a test system and a few selected buses as examples. In practice, system operators can run this analysis on various buses in their grid and complement steady-state system strength metrics with VVC to obtain a much broader picture of all system strength dimensions relevant to preserving dynamic security.

5. VVC interpolation considering parameter uncertainty

For a dynamic analysis of modern power systems to be as informative and accurate as possible, IBR, DER, and load models need to be parameterized well. This can be naturally a difficult task, particularly for medium and low voltage levels where data availability and quality are not always sufficient. To tackle this challenge, the VVC method is hereby expanded to consider parameter uncertainty.

As presented in Section 3, the interpolation technique is used to derive voltage vulnerability curves from discrete simulation results. So far in the analysis, it was assumed that all the parameters are deterministically known, and simple linear interpolation was further used. As parameter uncertainty becomes a challenge, an advanced interpolation method called Locally Weighted Scatterplot Smoothing (LOWESS) is hereby introduced. This is followed by its utilization in voltage vulnerability curves to effectively tackle the parameter uncertainty challenges.

5.1. Interpolation with Locally Weighted Scatterplot Smoothing (LOWESS)

Locally Weighted Scatterplot Smoothing (LOWESS) is a statistical non-parametric regression method designed to combine multiple regression models in one. The core methodology is based on the k-closest samples. It falls into the broader category of predictive analytics

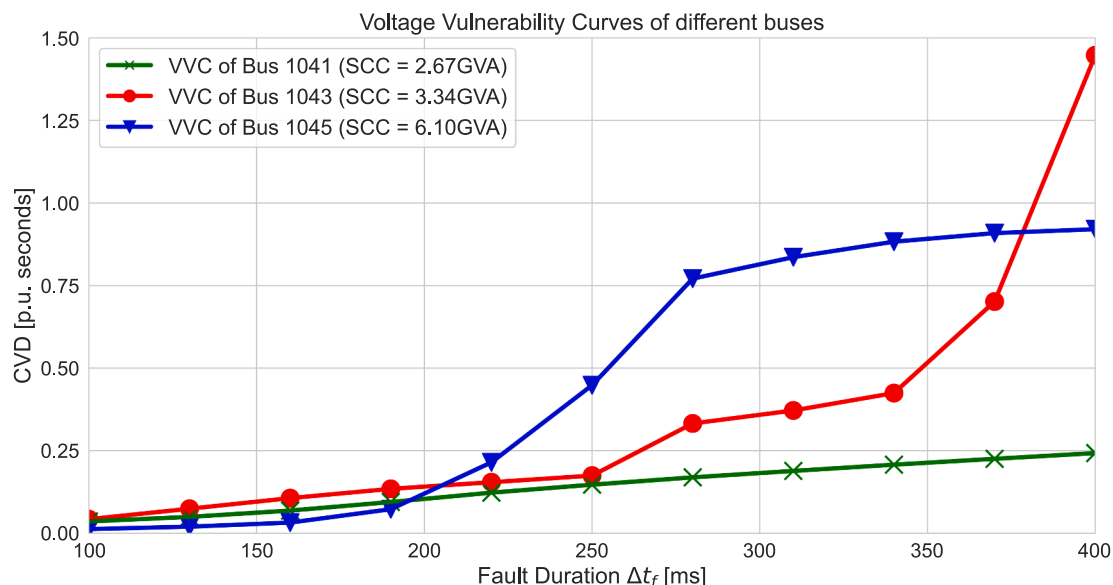


Fig. 19. Voltage Vulnerability Curves of buses 1041, 1043, and 1045 as per the test model in Fig. 17 and responses in Fig. 18.

methods designed for extrapolation or interpolation of data, as well as local regressions for robustly fitting smoothing curves without prior assumptions about the curve shape. LOWESS fundamentally relies on classical methods such as linear and nonlinear least squares regressions. However, it differs as it uses only subsets of data for each weighted least squares fit. In other words, it combines the results of multiple local regressions over different regions of the data domain based on weightings linked to the distance between the prediction point and the data used to fit each of the local regressions. Fig. 20 illustrates the LOWESS concept [51,52]. A regression is performed using a polynomial function on a local data subset centered around a particular. The procedure can be repeated multiple times to minimize the impact of outliers and obtain a more accurate result.

LOWESS is a non-parametric regression method, hence no analytical response function is produced. Instead, the predictor curve is data-driven and directly constructed according to the information derived from the data. It is therefore an effective method for cases where the data does not closely follow any clear analytical pattern, such as with noisier and scattered data with a complex relationship, and where the analytical function is not suitable or necessary. A comprehensive discussions on the LOWESS algorithm, its applications, limitations, and parametrization are out of the scope of this paper and can be found in [51–53].

Once all the local regressions are derived using a moving localized regression approach, the final LOWESS curve is created, as depicted in the thick pink line in Fig. 20. This final curve, however, only indicates the mean prediction value of the algorithm. To include uncertainty prediction intervals around it, MOE-Py implementation of the LOWESS method is utilized here [53], as part of the scripting within the DSA described in Fig. 7. The implementation of LOWESS for VVC curves interpolation that considers uncertainty is hereby further demonstrated.

5.2. Evaluating parameter uncertainty impacts with LOWESS and voltage vulnerability curves

Voltage Vulnerability Curves are fundamentally data driven. A series of scattered CVD values are derived from simulations, with a discrete fault time step between them, selected to balance the trade-off of speed and accuracy. To produce a continuous curve that provides complete insights, an interpolation technique can be applied. In the analysis so far, linear interpolation was used (e.g. Fig. 19). This is naturally a simple approximation, and more importantly, such interpolation is not able to consider parameter uncertainty. To expand on this, LOWESS interpolation is hereby utilized to enhance the VVC method. To demonstrate this,

the system from Fig. 17 is adjusted to incorporate dynamic loads in bus 1041. The D-type motors are used, which stall for longer fault duration and initiate FIDVR events.

Two parameters chosen to represent the uncertainty are the penetration of the D-type motor in the WECC composite load model ($F_{m,d}$) and the thermal time constant of the motors (T_{th}) which affects the stalling characteristics. These parameters are selected due to their large impact on FIDVR intensity, as reported in [54,55,8]. Furthermore, fault duration is increased in steps of 25 ms from 100 ms to 400 ms, with an additional small randomness around it.

The uncertainty of the parameters is modelled by randomly sampling from a normal distribution in each simulation, as shown in Fig. 21. There are, of course, many more advanced ways to model parameter uncertainty depending on the application and goal, which is beyond the scope of this work [56–58]. Instead, the goal here is to demonstrate how any parameter uncertainty model can be effectively incorporated into the VVC methodology.

The resulting family of 90 curves showing voltage responses with parameter uncertainty are plotted in Fig. 22. As seen from the curves, the wide parameter uncertainty reflects itself in a wide dispersion of voltage deviations with varying severity. In other words, the selected parameters and their wide range have a large impact on the voltage deviations of this busbar following the same disturbance.

The VVC curve is created based on the simulation results and plotted in Fig. 23, relative to the static load scenario. The simulation results are shown in blue dots, based on their respective CVD and Δt_f values. Afterwards, the simulation results are utilized for regression and interpolation using the described LOWESS method. The mean value is plotted (black curve), alongside two prediction intervals to capture the uncertainty of the parameters and illustrate their impact on voltage vulnerability curves.

As seen from Fig. 23, the results for < 200 ms fault duration are very much in line with the linear static load curve. The mean prediction matches the static load profile curve, and uncertainty intervals are very narrow. Hence, the dynamic strength is not influenced by the demand composition and its parameter uncertainty for shorter-duration faults.

However, as fault duration increases, voltage deviations become more severe. Furthermore, the uncertainty intervals also widen, as indicated by the two shaded areas. This is expected, as more severe faults reveal the impact of dynamic load parameters more strongly.

The information provided by such a curve can help grid operators evaluate the dynamic-state system strength and estimate the risk of short-term instabilities for not just varying fault duration, but also for a broad range of parameters of relevance considering their uncertainty in dynamic grid models across varying operating conditions.

6. Conclusions

Maintaining voltage stability and sufficient system strength are some of the key challenges in the operation of modern power systems. Both aspects have been evolving together with power systems, raising the need for more advanced understanding and evaluation methods. This paper provided an extensive theoretical and analytical discussion of these two challenges, where new definitions and classifications are proposed and discussed. Furthermore, an advanced novel quantification method is proposed, voltage vulnerability curves, to tackle some of the discussed challenges. The method is also expanded to consider the parameter uncertainty of numerous IBRs and loads in a grid.

The method can be implemented as a part of the probabilistic dynamic security assessment, with a focus on short-term instabilities and the risk of cascading events. In this way, grid operators can get advanced insights from RMS simulations into not only static grid limitations but also dynamic system behavior in terms of the likelihood of short-term instabilities. For each grid location of interest, a quantitative steady-state system strength value can be complemented by a respective VVC, representing a dynamic-state system strength quantification for the

LOWESS: 1st-order weighted local regression
key parameter: fraction

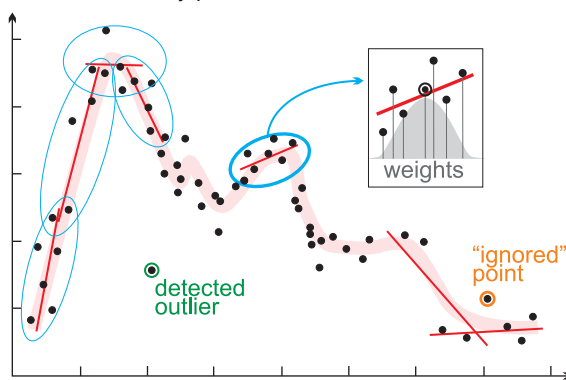


Fig. 20. Principles of LOWESS for a 1st-order polynomial. Black points are the source data; red narrow lines are the local regression solutions; the thick rose line is the final LOWESS solution. The grey area on the sub-panel represents a weight-defining function.

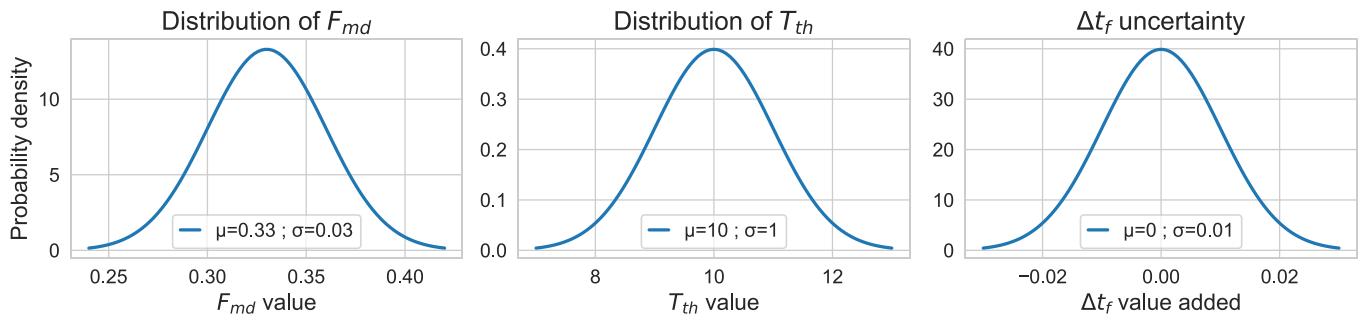


Fig. 21. Uncertainty modelling of the three selected parameters using a normal distribution with mean value (μ) and standard deviation (σ).

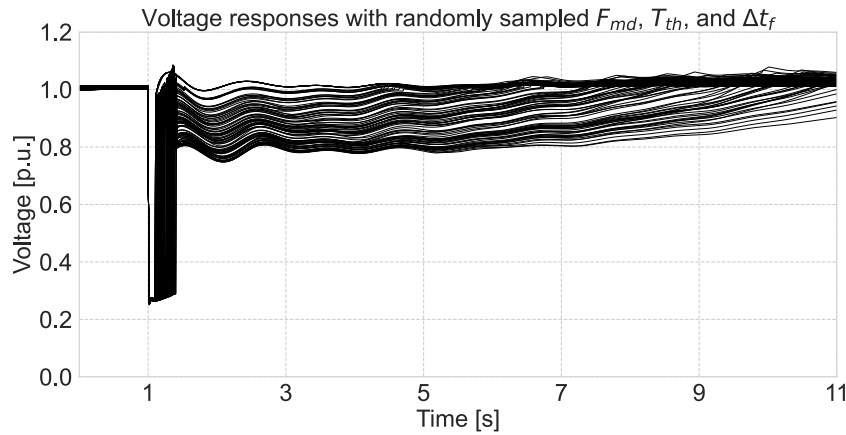


Fig. 22. Voltage responses of bus 1041 with considering broad parameter uncertainty.

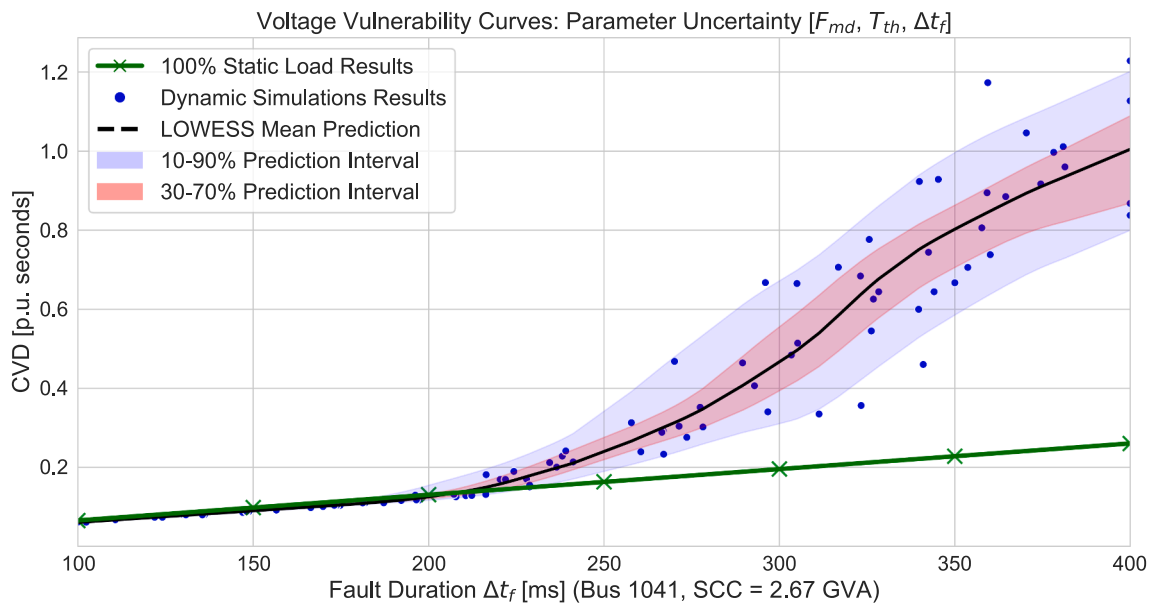


Fig. 23. VVC of results from Fig. 22 with parameter uncertainty modelled with the LOWESS method.

selected disturbances and parameters. The result is an automated vulnerability assessment across both steady- and dynamic-state operations, indicating which grid locations exhibit relative voltage weakness and risk of instability. Once detected, such operational scenarios can be directly avoided or explored further with detailed analysis and resolved with mitigation measures in a much more time-efficient manner.

In future work, the authors will demonstrate the efficacy and usefulness of the method to locate weak buses in an actual large-scale

transmission network in the Netherlands, where quantitative instability risk levels can be further evaluated, as well as the efficacy of mitigation actions. Furthermore, combined steady- and dynamic-state system strength assessment will be explored, to effectively quantify multiple dimensions of modern power systems' voltage resilience and vulnerability and offer advanced system strength analytics to grid operators. Lastly, improvements to the methodology by using AI and machine learning may be another promising future research direction to

explore.

CRedit authorship contribution statement

Aleksandar Borčić: Writing – original draft, Visualization, Methodology, Investigation, Formal analysis, Data curation, Conceptualization. **Marjan Popov:** Writing – review & editing, Supervision, Funding acquisition, Conceptualization.

Declaration of competing interest

The authors declare that they have no known competing financial

Appendix

The IEEE Test System for Voltage Stability Analysis and Security Assessment can be downloaded from the following link: <https://cmte.ieee.org/pes-psdp/489–2/>.

All the parameters and details of the original system from Fig. 4 can be found in [35,42].

Table 1 describes parameters used to exemplify various dynamic effects of DER units and dynamic loads that can be successfully captured by the newly proposed method.

Table 1
Parameters relevant for simulations in Sections 4 and 5. ($\Delta t_f = [100\text{--}400]$ ms).

Figure	Load	LV-DER	MV-DER
Fig. 12.	$F_{md} = 0.33$ $V_{st} = 0.5$ $T_{th} = 10$, $T_{sr} = 0.1$	N/A	N/A
Fig. 14.	Default values	$P = 600$ $V_{fr} = [1 - 0]$	$P = 200$ $V_{l0} = 0.5$, $t_{vl0} = 0.33$
Fig. 17 (a)	Default values	$P = 100$	– $P_{1,2} = 300$ $V_{(l0)1,2} = 0.5$ $t_{(vl0)1,2} = 0.352/0.2$
Fig. 17. (b)	Default values	N/A	
Fig. 17. (c)	$P_1 = [720 - 144]$ $P_2 = 720 - P_1$ $F_{md} = 0.3$ $V_{(st)1,2} = 0.2/0.7$ $T_{(st)1,2} = 0.5/0.2$ $T_{(th)1,2} = 10/20$	$P = 500$ $V_{l0} = 0.6$, $t_{vl0} = 0.5$ $V_{l1} = 0.9$, $t_{vl1} = 0.4$ $V_{fr} = [1 - 0.5]$	N/A

Other load and DER parameters are kept at their default DigSILENT PowerFactory values, which can be found in PowerFactory templates of the WECC Composite Load model and DER_A model, respectively. The utilized parameters are illustrative only and do not represent any specific generation or load units or grid code requirements.

All simulations are performed on a Windows 10 PC, with Intel Xeon W-2123 3.6 GHz CPU and 8 GB of RAM.

Data availability

Data will be made available on request.

References

- [1] IEA. Renewables 2023, Analysis and forecasts to 2028. Technical report. Paris: International Energy Agency; 2023.
- [2] NERC. An introduction to inverter-based resources on the bulk power system. North American Electric Reliability Corporation; 2023.
- [3] Milano F, Dorfler F, Hug G, et al. Foundations and challenges of low-inertia systems (invited paper). Power systems computation conference (PSCC). IEEE; 2018.
- [4] Kenyon RW, Bossart M, Markovic M, et al. Stability and control of power systems with high penetrations of inverter-based resources: An accessible review of current knowledge and open questions. Sol Energy 2020.
- [5] Entso-e. Dynamic security assessment (DSA). SPD DSA Task Force; 2017.
- [6] Milanovic JV, Yamashita K, Martinez Villanueva S, et al. International industry practice on power system load modeling. IEEE Trans Power Syst 2013.
- [7] Arif A, Wang Z, Wang J, et al. Load modeling — a review. IEEE Trans Smart Grid 2018.
- [8] Borčić A, Torres JLR, Popov M. Fundamental study on the influence of dynamic load and distributed energy resources on power system short-term voltage stability. Int J Electr Power Energy Syst 2021.
- [9] CIGRE WG C4.56. Electromagnetic transient simulation models for large-scale system impact studies in power systems having a high penetration of inverter-connected generation. Tech. rep. CIGRE; 2022.
- [10] IEEE. Computer simulation tools. IEEE Electrif Mag 2023.
- [11] IEEE. Inverter-based resources (IBRs), status, opportunities, and challenges. IEEE Power Energy Mag 2024.
- [12] Ramasubramanian D, Pourbeik P, Farantatos E, Gaikwad A. Simulation of 100% inverter-based resource grids with positive sequence modeling. IEEE Electrif Mag 2021.
- [13] Ramasubramanian D, Wang X, Goyal S, et al. Parameterization of generic positive sequence models to represent behavior of inverter-based resources in low short circuit scenarios. Electr Power Syst Res 2022.
- [14] Borčić A. Vulnerability assessment of modern power systems: voltage stability and system strength perspectives. PhD Thesis. TU Delft; 2024.
- [15] Hatzigiorgiou N, Milanovic J, Rahmann C, et al. Definition and classification of power system stability – revisited & extended. IEEE Trans Power Syst 2021.
- [16] Taylor WC. Power system voltage stability. McGraw-Hill; 1994.
- [17] Cutsem T, Vournas C. Voltage stability of electric power systems. Boston, MA: Springer, US; 1998.
- [18] Matevosyan J, et al. A future with inverter-based resources. IEEE Power Energy Soc: Future Balanc Act - High VRE Penetr Energy Syst Integr 2021.
- [19] CIGRE JWG C4/C2.58/IEEE. Evaluation of voltage stability assessment methodologies in modern power systems with high penetration of inverter-based resources; 2024.

- [20] IEEE PES-TR77. Stability definitions and characterization of dynamic behavior in systems with high penetration of power electronic interfaced technologies. IEEE Power Energy Soc 2020.
- [21] Borčić A, Torres JLR, Popov M. Comprehensive review of short-term voltage stability evaluation methods in modern power systems. *Energies* 2021.
- [22] NERC. Integrating inverter-based resources into low short circuit strength systems - reliability guideline. Technical report. North American Electric Reliability Corporation; 2017.
- [23] Badrzadeh B, Emin Z, Goyal S, et al. System strength. *CIGRE Sci Eng J* 2021.
- [24] National Grid. System operability framework. Tech. rep.; 2014.
- [25] MIGRATE Project. Massive integration of power electronic devices. Tech. rep.; 2019.
- [26] AEMO. System strength in the NEM explained. Tech. rep. Australian Energy Market Operator; 2020.
- [27] Borčić A. Impact on power system protection by a large penetration of renewable energy sources. Master Thesis. Eindhoven University of Technology; 2019.
- [28] Haddadi A, Farantatos E, Kocar I, Karaagac U. Impact of inverter based resources on system protection. *Energies* 2021.
- [29] Torzkadeh R, Waes J, Mulder G, et al. An estimation for short-circuit power changes in the Dutch grid to analyze the impacts of energy transition on voltage dips. Paris: CIGRE; 2022.
- [30] Borčić A, Torres JLR, Popov M. System strength: classification, evaluation methods, and emerging challenges in IBR-dominated grids. *IEEE PES innovative smart grid technologies (ISGT) - Asia*. 2022.
- [31] Zhu Y, Green TC, Zhou X, et al. Impedance margin ratio: a new metric for small-signal system strength. *IEEE Trans Power Syst* 2024.
- [32] CIGRE WG B4.62 671. Connection of wind farms to weak AC networks. Tech. rep. CIGRE; 2016.
- [33] Borčić A, Torres JLR, Popov M. Beyond SCR in weak grids: analytical evaluation of voltage stability and excess system strength. *International conference on future energy solutions (FES)*. IEEE; 2023.
- [34] NERC. Integrating inverter-based resources into low short circuit strength systems - reliability guideline. North American Electric Reliability Corporation; 2017.
- [35] Pes IEEE, Ieee pes-tr19,. Test systems for voltage stability analysis and security assessment. Tech. rep. IEEE Power & Energy Society; 2015.
- [36] Lew D, Asano M, Boemer J, et al. The power of small: the effects of distributed energy resources on system reliability. *IEEE Power Energy Mag* 2017.
- [37] Borčić A, Torres JLR, Popov M. Quantification and classification of short-term instability voltage deviations. *IEEE Trans Ind Appl* 2023.
- [38] Borčić A, Torres JLR, Popov M. Quantifying the severity of short-term instability voltage deviations. *International conference on smart energy systems and technologies (SEST)*. 2022.
- [39] Zubic S, Gajic Z, Kralj D. Line protection operate time: how fast shall it be? *IEEE Access* 2021.
- [40] ENTSO-e Requirements for Generators (RfG), Commission Regulation (EU) 2016/631.
- [41] Borčić A, Torres JLR, Popov M. Impact of modelling assumptions on the voltage stability assessment of active distribution grids. *IEEE PES innovative smart grid technologies (ISGT) Europe*. 2020.
- [42] Van Cutsem T, Glavic M, Rosehart W, et al. Test systems for voltage stability studies. *IEEE Trans Power Syst* 2020.
- [43] WECC Dynamic Composite Load Model (CMPLDW) Specifications. Tech. rep. Iowa State University; 2015.
- [44] Adhikari S, Schoene J, Gurung N, Mogilevsky A. Fault induced delayed voltage recovery (FIDVR): modeling and guidelines. *IEEE Power & Energy Society General Meeting (PESGM)*. 2019.
- [45] Hajipour E, Saber H, Farzin N, Karimi MR, Hashemi SM, Agheli A, et al. An improved aggregated model of residential air conditioners for FIDVR studies. *IEEE Trans Power Syst* 2020.
- [46] IRENA. Grid codes for renewable powered systems, International Renewable Energy Agency. Tech. rep. Abu Dhabi: International Renewable Energy Agency; 2022.
- [47] NERC. Reliability guideline modelling distributed energy resources in dynamic load models. Tech. rep. North American Electric Reliability Corporation; 2016.
- [48] NERC. Distributed energy resources connection modelling and reliability considerations. Tech. rep. North American Electric Reliability Corporation; 2017.
- [49] Ma Z, Wang Z, Wang Y, Diao R, Shi D. Mathematical representation of WECC composite load model. *J Mod Power Syst Clean Energy* 2020.
- [50] AEMO. Behaviour of distributed resources during power system disturbances: Overview of key findings. Tech. rep. Australian Energy Market Operator; 2021.
- [51] Cleveland WS. Robust locally weighted regression and smoothing scatterplots. *J Am Stat Assoc* 1979.
- [52] Derkacheva A, Mougnot J, Millan R, et al. Data reduction using statistical and regression approaches for ice velocity derived by landsat-8, sentinel-1 and sentinel-2. *Remote Sensing* 2020.
- [53] Bourn A. Merit-order-effect (MOE-Py) python library; 2021.
- [54] Tenza MW, Ghiocel S. An analysis of the sensitivity of WECC grid planning models to assumptions regarding the composition of loads. Tech. rep. Mitsubishi Electric Power Products; 2016.
- [55] Nuthalapati S. Use of voltage stability assessment and transient stability assessment tools in grid operations. Springer International Publishing; 2021.
- [56] Hasan K, Preece R, Milanović J. Existing approaches and trends in uncertainty modelling and probabilistic stability analysis of power systems with renewable generation. *Renew Sustain Energy Rev* 2019.
- [57] Hakami A, Hasan K, Alzubaidi M, et al. Review of uncertainty modelling techniques for probabilistic stability analysis of renewable-rich power systems. *Energies* 2022.
- [58] Singh Vikas, Moger Tukaram, Jena Debashisha. Uncertainty handling techniques in power systems: A critical review. *Electr Power Syst Res* 2022.